



ÉCOLE POLYTECHNIQUE FÉDÉRALE DE
LAUSANNE

Optomotor Turning in NeuroMechFly: a Connectome-Constrained Approach

Abstract – In this report, we explore the integration of a connectome-constrained deep neural network with the biomechanical model NeuroMechfly 2.0 to simulate visually elicited behaviors of the adult fruit fly *Drosophila melanogaster*. Our study primarily addresses the fly’s optomotor response through an analysis of underlying neural activity patterns produced by the network. Through the use of rotating drums with alternating black and white stripes, we demonstrate that the network, previously optimized for optic flow computation, can generate activity patterns close to reality, as found in the litterature. In particular, based on those neural responses, we have constructed a controller to induce an optomotor turning in the model of the fly in real time, ressembling the optomotor behavior of biological flies. This study also discusses the potential limitations of the neural network in generating purely realistic neuronal patterns, and provides new strategies to produce more biologically realistic behaviors in the fly’s model, such as integrating escape responses to looming stimuli. The GitHub repository containing the code used in this study as well as complementary videos can be found [here](#).

Keywords – *NeuroMechFly*, *Optomotor response*, *Adult fly Drosophila melanogaster*, *Connectome-constrained neural network*.

BIOENG-456 – CONTROLLING BEHAVIOR IN ANIMALS AND ROBOTS

Nils Antonovitch
Viva Berlenghi
Florian David

24th May 2024

Contents

1	Introduction	2
1.1	Literature survey	2
1.1.1	NeuroMechFly	2
1.1.2	Fly visual system	2
1.1.3	Optic flow and motion detection	4
1.1.4	Optomotor response and other behavioral responses to visual stimuli	5
1.1.5	Connectome-constrained neural network	5
1.2	Motivations and goals	7
2	Methods	7
2.1	The fly	7
2.2	The arenas	7
2.2.1	Rotating striped drum	7
2.2.2	Approaching object	9
2.3	The optomotor controller	10
3	Results	12
3.1	Neuron tuning to different visual stimuli when the fly is fixed	12
3.1.1	Rotating striped drum	12
3.1.2	Approaching object	15
3.2	Optomotor response in real time (large-field rotating stimuli)	16
4	Discussion	17
4.1	The adaptative controller yields better results than the all-or-none controller . .	17
4.2	Only a few neurons are required to generate complex behaviors	18
4.3	Directional bias for leftward motion	18
4.4	Angular velocity limits	18
4.5	Looming stimuli	19
4.6	Anti-directional turning	20
5	Conclusion	20

1 INTRODUCTION

1.1 LITERATURE SURVEY

1.1.1 NEUROMECHFLY

NeuroMechFly 2.0 is an advanced simulation framework developed to model the neuromechanical aspects of the adult fly *Drosophila melanogaster* [1]. It allows detailed simulations of sensorimotor behavior in a three-dimensional environment, as well as biomechanical modeling with sensory processing, decision-making, and motor execution (see Fig. 1). It represents an enhancement from its predecessor [2] with the added rugged terrain, visual object chasing, and olfactory-driven behaviors.

It presents multiple key features; biomechanical modeling, for instance, allows for an anatomically accurate representation of the fly and requires precise configurations of leg joints and body segments. Leg adhesion mechanics are also an important element, taking into account the adhesive properties of the fly's legs, thus enabling it to navigate across various surfaces with a range of inclinations. The framework is also conveniently compatible with reinforcement learning algorithms, which allows researchers to gain new insights regarding decision-making in biological systems. Additionally, it is able to realistically simulate sensory inputs from the retina for vision and from the antennae and maxillary palps for olfaction, thus integrating both visual and chemical signals.

The visual system will mostly be used in this project. It is a particularly advanced model, with 721 cameras representing compound eyes in an ommatidial manner, and it has been trained to track and respond to visual stimuli dynamically.

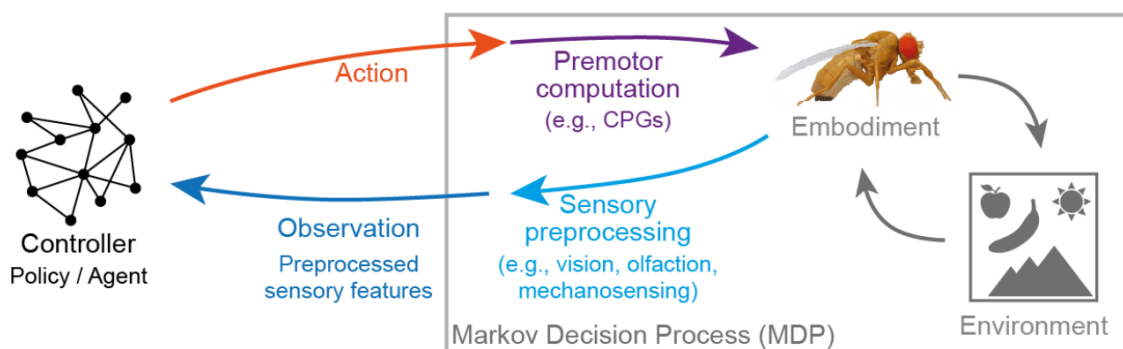


FIGURE 1
Schematic overview of the NeuroMechFly 2.0 modeling framework. A Markov Decision Process (MDP) task encapsulates the biomechanical model of the fly as well as its interaction with the environment. A user-defined controller interfaces with the task through actions (red) and observations (blue). This figure was extracted from [1].

1.1.2 FLY VISUAL SYSTEM

The visual system of the adult fly *Drosophila melanogaster* has been studied extensively in the past [3–6]. With a limited number of neurons capable of generating complex behaviors, the brain of the fly is a great model for understanding visual processing (see Fig. 2). This system is composed of several interconnected regions, namely the retina, lamina, medulla, lobula, and

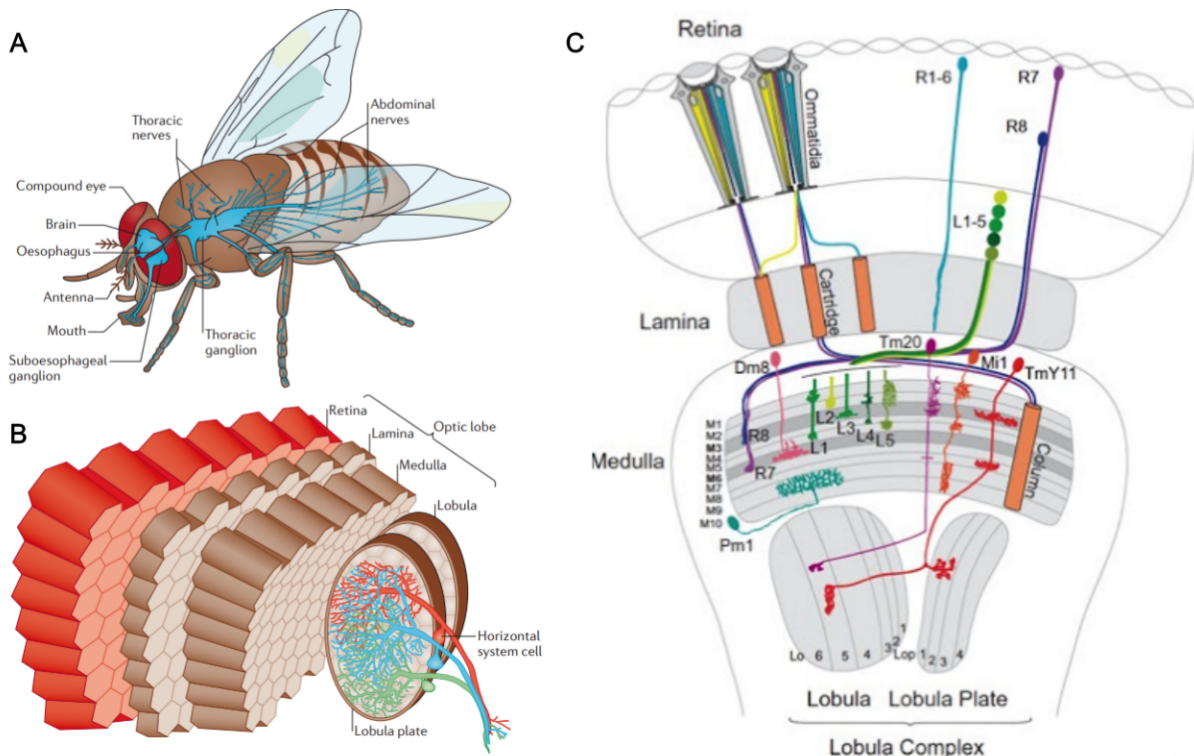


FIGURE 2

The fly's visual system. **A|** The fly's nervous system is divided between the brain and the thoracic ganglion. **B|** The eye of the fly consists of many hundreds of facets (in red) called ommatidia, each containing photoreceptors. They send their axons into the optic lobes (one on each side of the head), which include the major part of the head ganglion. Each lobe consists of four retinotopically arranged neuropil layers, which are called the lamina, medulla, lobula, and lobula plate. Horizontal system cells respond to large-field horizontal motion, as occurs during rotation of the fly around the vertical body axis, and are involved in corrective steering maneuvers. **C|** Illustration representing the main different types of neurons in the optic lobe and their synaptic organization and relationship. A and B were taken from [5], whereas C can be found in [4].

lobula plate, each playing different roles, with higher-level areas processing more complex features of visual stimuli.

The retina contains multiple photoreceptor cells (R1 to R8) organized into ommatidia, which constitute the fly's compound eye. These cells capture light and colors and are either connected to the lamina (R1 to R6 involved in motion detection) or to the medulla (R7 and R8 involved in detail perception). The lamina is organized into a retinotopic map, maintaining the spatial arrangement of the photoreceptors, and sends projections to the medulla for further processing of the visual information. The medulla, the largest visual processing center in the fly's brain, is divided into ten layers, with each column containing more than 60 different cell types, such as medulla intrinsic (Mi) and trans-medulla (Tm) neurons. Finally, further processing is carried out in the lobula complex, which is also divided into multiple layers. Tm neurons link the medulla to the lobula and the lobula plate through T4 and T5 neurons, known to be tuned to different motion directions (see Fig. 3). Altogether, this network houses several pathways, giving rise to visually elicited complex behavioral responses.

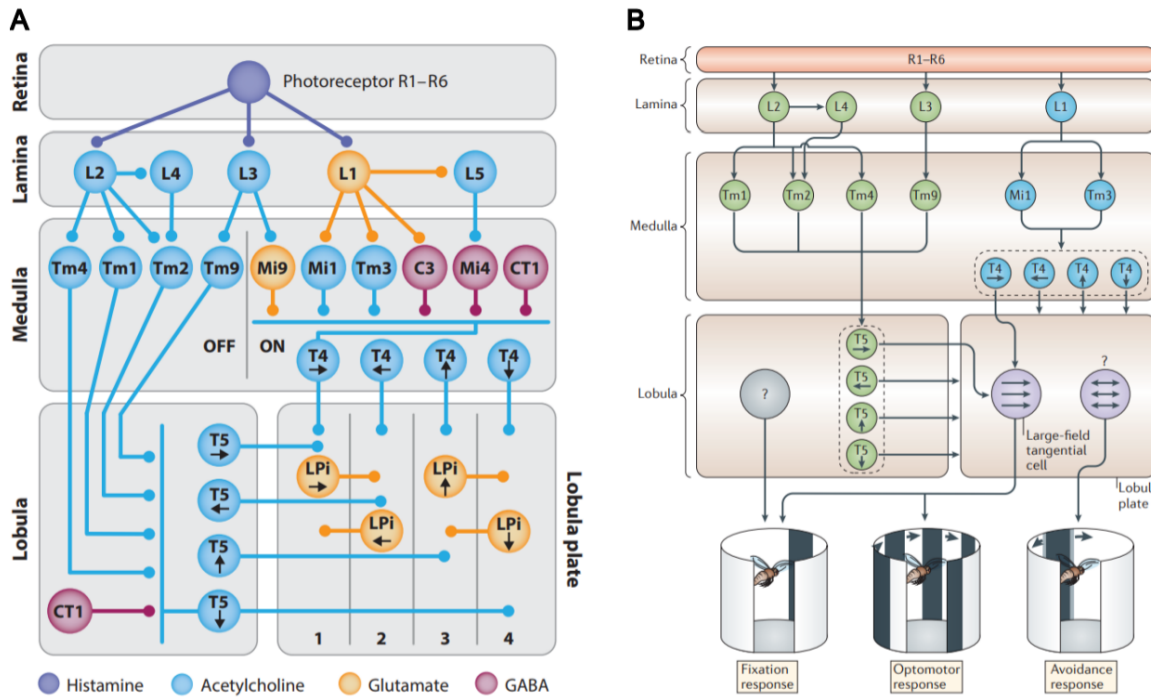


FIGURE 3

Diagrams of the motion vision circuit. Photoreceptors connect to lamina (L) cells that split signals into an ON and an OFF pathway. Transmedullary (Tm), medulla intrinsic (Mi), centrifugal (C), and complex tangential (CT) cells relay temporally filtered signals to the dendrites of T4 cells in the medulla and of T5 cells in the lobula. Different types of T4 and T5 cells send their axons to one out of four layers of the lobula plate, where they synapse onto lobula plate intrinsic (LPi, only represented in A) and lobula plate tangential cells (only represented in B). Some connections and cell types have been omitted for clarity. B also shows neural circuits underlying fixation, optomotor, and avoidance responses. Both figures were taken from [5, 6].

1.1.3 OPTIC FLOW AND MOTION DETECTION

Motion detection in insects is crucial for navigation in complex environments, predator avoidance, prey hunting, and many other behaviors. For this, the fly computes optical flow: "the pattern of apparent motion of objects, surfaces, and edges in a visual scene caused by the relative motion between an observer (an eye or a camera) and the scene" [7]. In particular, T4 and T5 are motion-direction selective neurons, and each can be divided into 4 subtypes, one per preferred direction (T4a to T4d and T5a to T5d). T4 and T5 correspond, respectively, to ON and OFF pathways: the ON pathway processes increase in light intensity (moving light edges), while the OFF pathway processes decrease in light intensity (moving dark edges) [6].

The computation of motion also depends on the spatial arrangement and the interplay of excitatory and inhibitory inputs to T4 and T5 cells, mainly subtypes of Tm and Mi neurons across the medulla. In particular, to improve the sensitivity to motion direction in T4 neurons, flies use a mechanism of multiplicative disinhibition. For example, when an object moves in the preferred direction of a T4a neuron (rightward), its inhibitory inputs are reduced (but not for other T4 subtypes), thus greatly increasing the responsiveness of this specific subtype cell to its excitatory inputs, which all remain constant (see Fig. 3A).

1.1.4 OPTOMOTOR RESPONSE AND OTHER BEHAVIORAL RESPONSES TO VISUAL STIMULI

The optomotor response is a stabilization strategy used by the fly during walking and flight, characterized by compensatory body movements congruent with the direction of the perceived motion with respect to the environment [8]. In other words, the fly aligns with the direction of moving visual patterns and allows it to maintain a straight trajectory in the presence of external disturbances. This behavioral response can be elicited when a large-field visual stimulus rotates around the fly, for example, while navigating near large objects in motion, and it can be triggered in simulations using a rotating striped drum [9].

The optomotor response relies not only on the integration of the visual inputs by T4 and T5 cells but also on computations performed by large tangential cells in the lobula plate, such as horizontal system (HS) cells [10]. They could be used to estimate self-motion while the fly changes coordinates and produces head movements. Indeed, it has been shown that optogenetic activation of those cells can induce optomotor turning [11].

Apart from the well-studied optomotor response, various visually guided behaviors triggered by different visual stimuli are performed by flies for navigation and survival (see Fig. 3B). First, an escape response can be elicited by a looming stimulus [12], perceived as a predator approaching. When the moving shadow reaches a specific angular size and velocity in its visual field (i.e., the object reaches a critical perceived size as it approaches), the fly escapes in the opposite direction [13]. It is worth noting that faster-expanding patterns will trigger quicker escape responses, as the critical perceived size will be reached sooner [14]. Second, similar to the escape response, the landing response is triggered by objects getting closer (i.e., increasing in size) but at slower velocities [15]. This behavior involves a complex sequence of actions for a smooth and controlled landing. Third, the fixation response is triggered by smaller, distinct objects and is used for mating or prey hunting, for example [16]. The fly uses those stimuli as targets not only to approach them but also to keep them at a constant visual angle (i.e., distance).

1.1.5 CONNECTOME-CONSTRAINED NEURAL NETWORK

In this study, we use a pre-trained neural network developed by [17] as a framework to control the behavior of the biomechanical fly model (see Fig. 4).

The architecture of the model reproduces the connectome of the *Drosophila melanogaster* visual system. It replicates the structural organization of the fly's visual system, where each unit of the network corresponds to an individual biological neuron. The researchers have included 64 distinct neuronal types, and they have defined synaptic weights as being proportional to experimentally determined synapse counts between pairs of presynaptic and postsynaptic neurons, with identical neuron pairs sharing the same properties. Among the neurons of the network, we find in particular T4 and T5 neurons, as well as several Tm neurons. The main advantage of having a connectome-constrained network is the ability to analyze individual neuron activity, allowing a deeper understanding of the visual computation at a single-neuron resolution.

The network was trained in a task-driven manner to compute optical flow from naturalistic videos, with the aim of reproducing the visual motion processing of the fly. Remarkably, although the model was not explicitly trained to optimize single neuron activity, the task-optimization approach enabled the emergence of natural neuronal pathways tuned to increases (ON) and decreases (OFF) in light intensities, as described in Section 1.1.2. In particular, the performance of the model in predicting single-neuron behaviors was assessed by comparing predictions to

experimental recordings.

As described in Section 1.1.1, the biomechanical model of the fly is able to simulate sensory inputs from the retina for vision. In other words, the fly can "see" its environment through 721 cameras per eye, corresponding to individual ommatidia. Therefore, we can feed those visual inputs to the pre-trained model, which, in return, outputs individual neuron responses. Then, based on the known properties of those neurons (such as ON and OFF tuning of T4 and T5 neurons, respectively), we can generate a set of behaviors to control the fly.

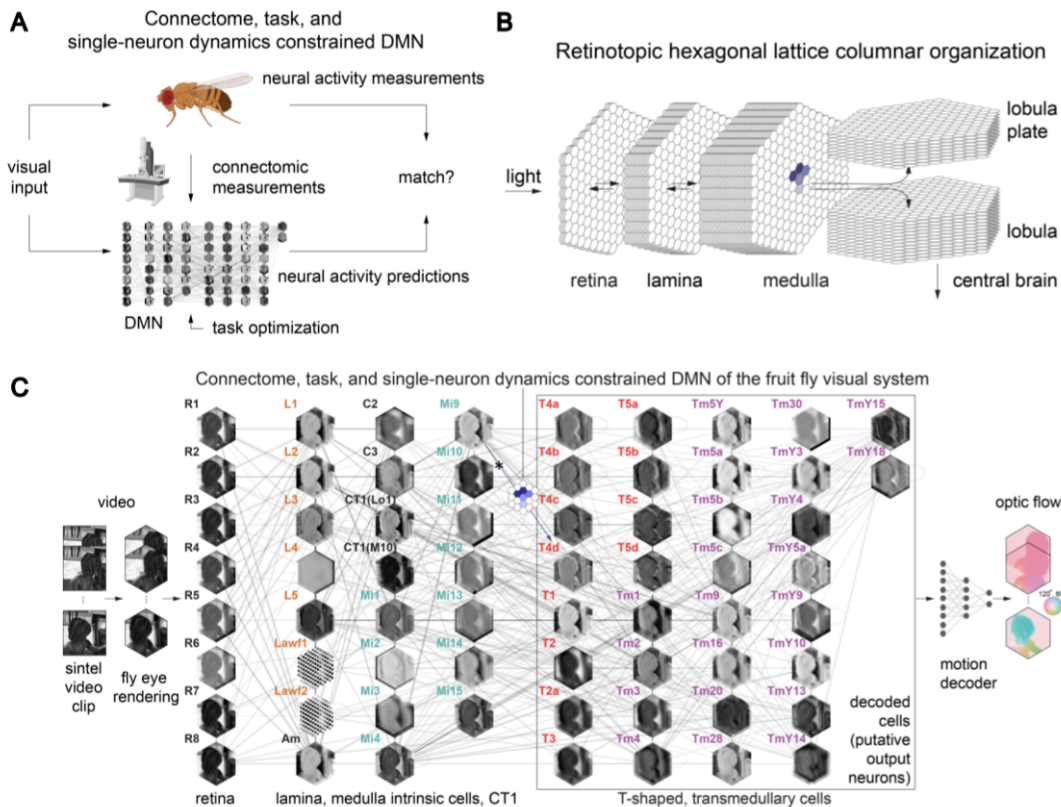


FIGURE 4

Connectome-constrained model of the fly visual system optimized on an optical flow computation task. **A|** The network aims to satisfy three constraints simultaneously: Its architecture is based on connectomic measurements, neuron properties are given by simple mechanistic models, and free parameters are optimized by training the model to perform an optic flow estimation task. **B|** Retinotopic hexagonal lattice columnar organization of the visual system model. Each lattice represents a cell type, and each hexagon represents an individual cell. The positions of photoreceptor columns are aligned with the positions of downstream columns. **C|** Visualization of the network performing optic flow estimation on a video clip rendered from the Sintel dataset. Each hexagonal lattice depicts a snapshot of the voltage levels of all cells from the corresponding cell type. Edges illustrate connectivity between identified cell types. This figure was adapted from [17].

1.2 MOTIVATIONS AND GOALS

In this study, we aim to explore the use of a connectome-constrained deep neural network to process visual information to elicit an optomotor turning in a biomechanical model of the *Drosophila melanogaster*. In particular, we will analyze neurons' responses to various motion stimuli, and we will discuss how the model can improve the realism of the fly's behaviors as well as its limitations.

2 METHODS

2.1 THE FLY

The fly model we use belongs to NeuroMechFly 2.0, the data-driven computational model of adult *Drosophila melanogaster* mentioned in Section 1.1.1. The connectome-constrained model has been taken from Lappalainen et al.'s implementation [17] and is described in Section 1.1.5.

The network was optimized to calculate the optic flow on 23 sequences of the computer-animated movie Sintel [18], each containing 20–50 frames at a rate of 24 Hz. The dataset provides the optic flow for each frame after the first of every sequence. Since the integration timestep used was 5 ms, corresponding to a sampling rate of about 200 Hz (about 10x the frame rate of the sequences), the input frames are resampled accordingly over time, and the optic flow is interpolated.

While attempting to replicate the optic flow estimation, the network obtains various weights and activities for the different neurons that compose it, thus generating the neural activity output for multiple neurons in the visual field (see Fig. 5). As mentioned in Section 1.1.3, T4a and T4b neurons, along with T5a and T5b, all show distinct pattern activations when motion occurs. The neuronal activities are then fed to the controller in order to obtain the appropriate reaction of the fly to the stimulus.

2.2 THE ARENAS

Because we wanted to present two different stimuli to the fly, we created two distinct arenas: one to trigger an optomotor response, the other to analyse the neural activities in response to a looming stimulus.

2.2.1 ROTATING STRIPED DRUM

The optomotor visual stimulus was presented to the fly in MuJoCo, a physics engine [19], as done in [1]. The stimulus shown was a rotating striped drum, which corresponds to a circle with a modulable diameter composed of 18 cylinders of alternating colors, here black and white (see Fig. 5A). The circle's angular velocity is modulable and ranges between 0 and 10 rad/s. The following calculations allow us to convert frequencies into the angular speed of the rotating drum (see Fig. 6).

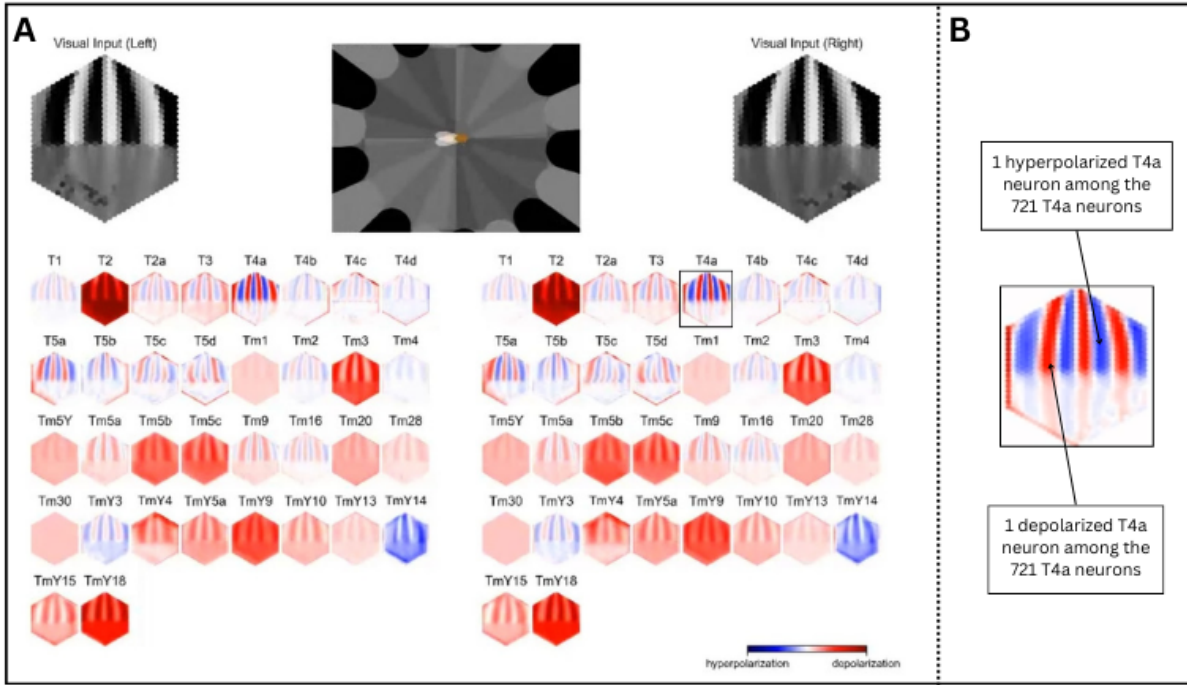


FIGURE 5

Rendering of the optomotor response simulation. **A|** Visual representation of the fly in its environment viewed from the top, what the fly sees in each eye, and neuronal activity (34 neuron types represented) in response to visual stimuli in real time based on the connectome-constrained network from [17]. **B|** Zoom in on one of the neuron types: T4a neurons linked to ommatidia from the right eye. Blue hexagons represent hyperpolarized neurons, while red hexagons represent depolarized neurons.

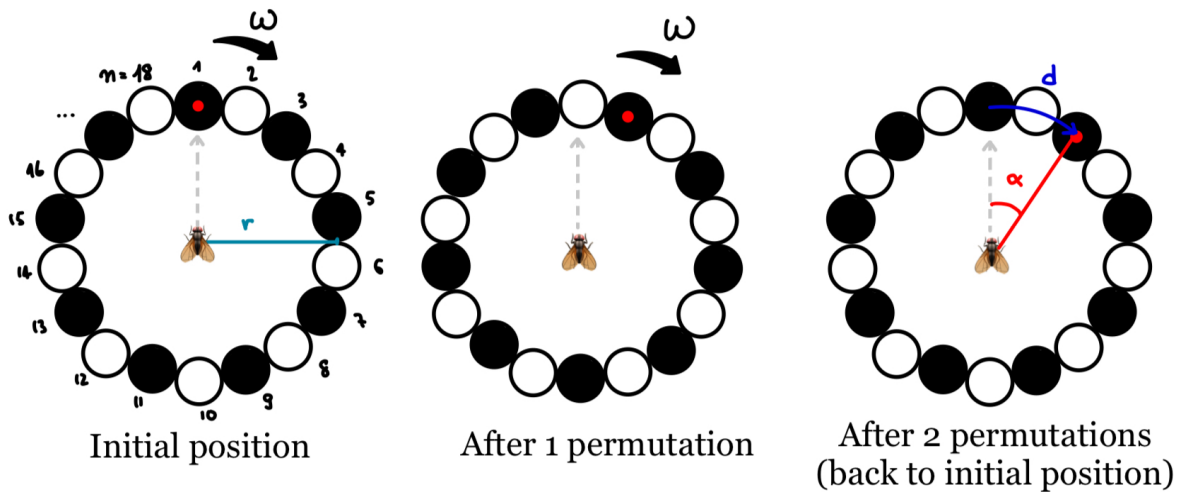


FIGURE 6

Arena scheme for two permutations. Black and white disks represent, respectively, black and white vertical stripes from the rotating drum.

As the frequency of a signal is the inverse of the amount of time it takes for the signal to reproduce itself, we can observe that this corresponds to two permutations (since we have two

alternating colors). We first need to obtain the angle that must be traveled by the strip drum (in radians) to undergo two permutations:

$$\alpha = \frac{2\pi}{n} \times 2 = \frac{4\pi}{n}$$

Knowing that the angular velocity ω is given, the time taken to execute two permutations is $T = \frac{\alpha}{\omega}$, and therefore the frequency of the stimulus is $f = \frac{1}{T} = \frac{\omega}{\alpha} = \frac{\omega n}{4\pi}$, and the angular velocity $\omega = \frac{4\pi f}{n}$. This means that, taking into account the frame rate of 200 Hz used to train the network, the neurons should be able to process visual information up to $\omega_{max} = \frac{4\pi \cdot 200}{18} \approx 139.62$ radians/second.

2.2.2 APPROACHING OBJECT

The looming visual stimulus consists of a black sphere approaching the fly (see Fig. 7). It is slightly off-center, so that it can be better seen by the left or right eye of the fly. The speed at which the ball moves toward or away from the fly is modulable. The sphere has a radius of 4 mm. It spawns 25 mm in front of the fly and 4 mm to its left. The rest of the implementation of the arena is unchanged.

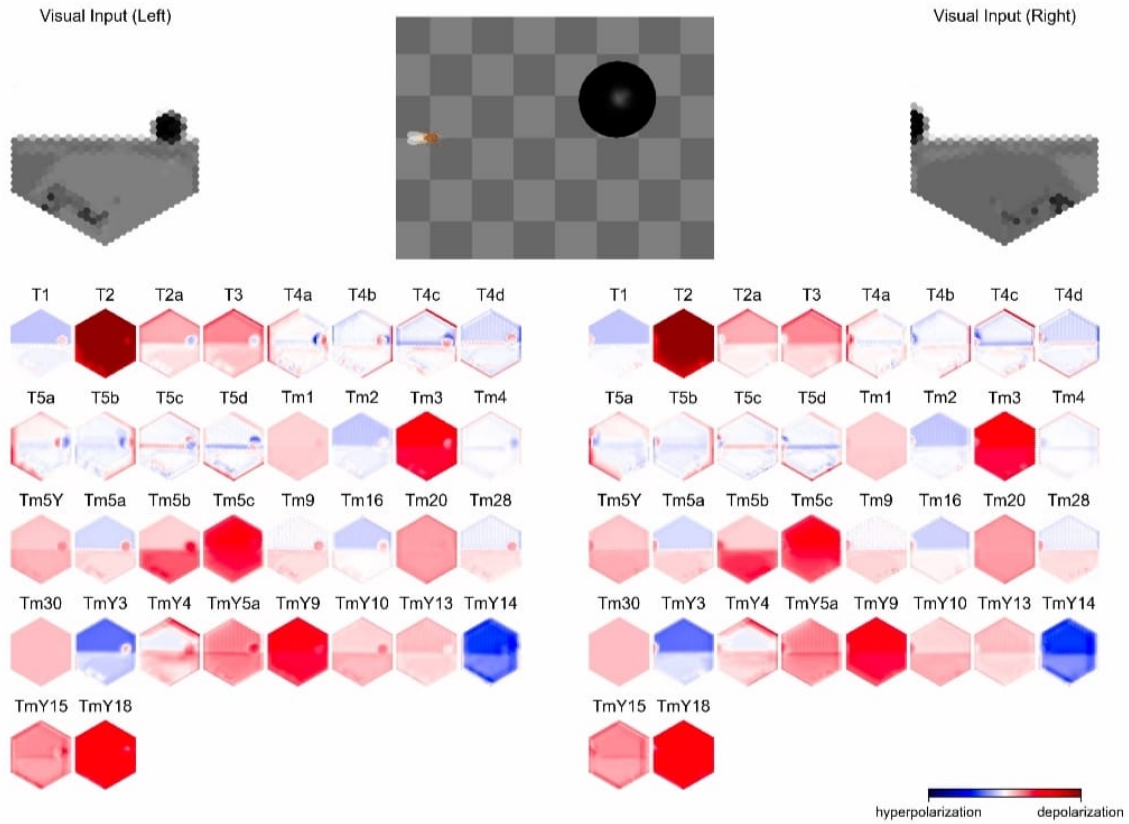


FIGURE 7

Rendering of the looming response simulation. Visual representation of the fly in its environment viewed from the top, what the fly sees in each eye, and neuronal activity (34 neuron types represented) in response to visual stimuli in real time based on the connectome-constrained network from [17].

2.3 THE OPTOMOTOR CONTROLLER

We aimed to build a controller to elicit a turning in the fly using neuronal patterns induced by a visual rotational stimulus. The neuronal activities are generated by the connectome-constrained model mentioned in the previous sections. While a detailed connectome of the visual system is described in figure 3A, the flyvis package only gives access to a subset of the represented neurons. Therefore, based on figure 3B, in the following we only consider:

- T4a and T4b neurons: these are part of the ON pathway and are motion-selective. T4a responds to an ON-edge moving from right to left (leftward), and T4b responds to an ON-edge going from left to right (rightward).
- T5a and T5b neurons: these are part of the OFF pathway and are motion-selective. T5a responds to an OFF-edge moving leftward, and T5b responds to an OFF-edge going rightward.
- Tm1, Tm2, Tm3, Tm4, and Tm9 neurons: these are some of the inputs to T4 and T5 neurons.

As the drum rotated, we observed important activity changes in T4 and T5 neurons. In

particular, because of ON and OFF tuning, at each time point, some of the 721 neurons were depolarized while others were hyperpolarized, depending on the localization of the ommatidia they are linked with (see Fig. 5B). As a result, it is possible to infer the direction and speed of the rotating stimuli by calculating the standard deviation (std) of those neurons across all ommatidia for each eye. Then, we have averaged the std values over both eyes as the visual inputs were the same but with a slight offset, which does not significantly affect the std values.

To test the individual roles of different neurons in this list, our controller can compute the turning bias based on any combination of activities from T4, T5, or Tm neurons. While the T4 and T5 neurons are used to detect the direction of the rotation of the environment, the Tm neurons are used as coefficients that multiply the activities of the T4 and T5 neurons. Based on their activity, we compute the turning strength of the fly and the angular speed at which the insect will turn. According to Section 1.1.3, it involves the activity of T4, T5, and several Tm neurons. We implement the turning strength as follows:

$$\text{turning_strength} = Kp \cdot ((T4a - T4b) \cdot Tm3 + (T5a - T5b) \cdot (Tm1 + Tm2 + Tm4 + Tm9)) \quad (1)$$

where Kp is a factor to make sure that the fly turns fast enough (empirically determined through an iterative process), and all other parameters correspond to the std of the neurons of interest across ommatidia at each time point, averaged over both eyes.

The equation 1 corresponds to the full implementation of the turning strength and depends on all the neurons of interest mentioned previously. However, we are also interested in simplified versions of the controller. Specifically, to only use T4 and T5 activities without considering Tm activities, we have set Tm3 and (Tm1+Tm2+Tm4+Tm9) values to 1 to obtain:

$$\text{turning_strength} = Kp \cdot ((T4a - T4b) + (T5a - T5b)) \quad (2)$$

Using the turning strength, we define the turning bias of the fly (combining both the direction and the strength). The turning bias is either adaptative (proportional to the turning strength) as:

$$\text{turning_bias} = [-\text{turning_strength}, \text{turning_strength}] * 1.2 \quad (3)$$

or defined in an all-or-none manner (depending on the sign of the turning strength) as:

$$\text{turning_bias} = [-\text{sign}(\text{turning_strength}), \text{sign}(\text{turning_strength})] * 1.2 \quad (4)$$

We chose a factor equal to 1.2 in equations 3 and 4 because any value larger than that might lead to an unstable gait. Overall, if the standard deviations of T4a and T5a neurons are greater than the standard deviations of T4b and T5b neurons, respectively, then the turning strength is positive, meaning that the fly will turn to the left. Conversely, if the standard deviations of T4b and T5b neurons are greater than the standard deviations of T4a and T5a neurons, respectively, then the turning strength is negative, meaning that the fly will turn to the right.

We have only implemented a controller to produce an optomotor response from the fly to rotating drums, but we have not implemented a controller to produce an escape response to a looming stimulus (an approaching object). We will later discuss some ideas for generating such a response according to the neuronal patterns observed.

3 RESULTS

We have analyzed the neuronal activity in response to different visual stimuli. At first, we keep the fly fixed while the environment evolves (see Section 3.1). Then, we have implemented the controller described in Section 2.2 to control the fly’s behavior in real-time (see Section 3.2). The first step was crucial to understanding how to implement the controller. Indeed, if the fly is not fixed, then it is complicated to identify and interpret neuronal patterns. At the end of each simulation, we store a .mp4 file to visualize the neuron activity and the fly’s behavior over time (for a rendering example, see Fig. 8), and we store a .pkl file containing all the neurons’ activity for further analysis. Some relevant videos can be found on the GitHub repository.

3.1 NEURON TUNING TO DIFFERENT VISUAL STIMULI WHEN THE FLY IS FIXED

3.1.1 ROTATING STRIPED DRUM

We can first visualize the evolution of the standard deviation of the different neurons of interest (see Fig. 8). Then, we can plot the evolution of the hypothetical turning bias strength and direction using the full equation 1 (see Fig. 9) or using the equation 2 without considering Tm neurons (see Fig. 10). The turning bias strength (black line) was calculated for different rotating drum speeds, but in the following, we will only consider a drum rotation speed v of 3 radians/second as it yielded the most valuable and interpretable results across all experiments. See also supplementary videos V1, V2, and V3 for a visual representation of neuronal activities with a drum rotating at a speed of, respectively, 1, 3, and 5 radians/second when the fly is fixed.

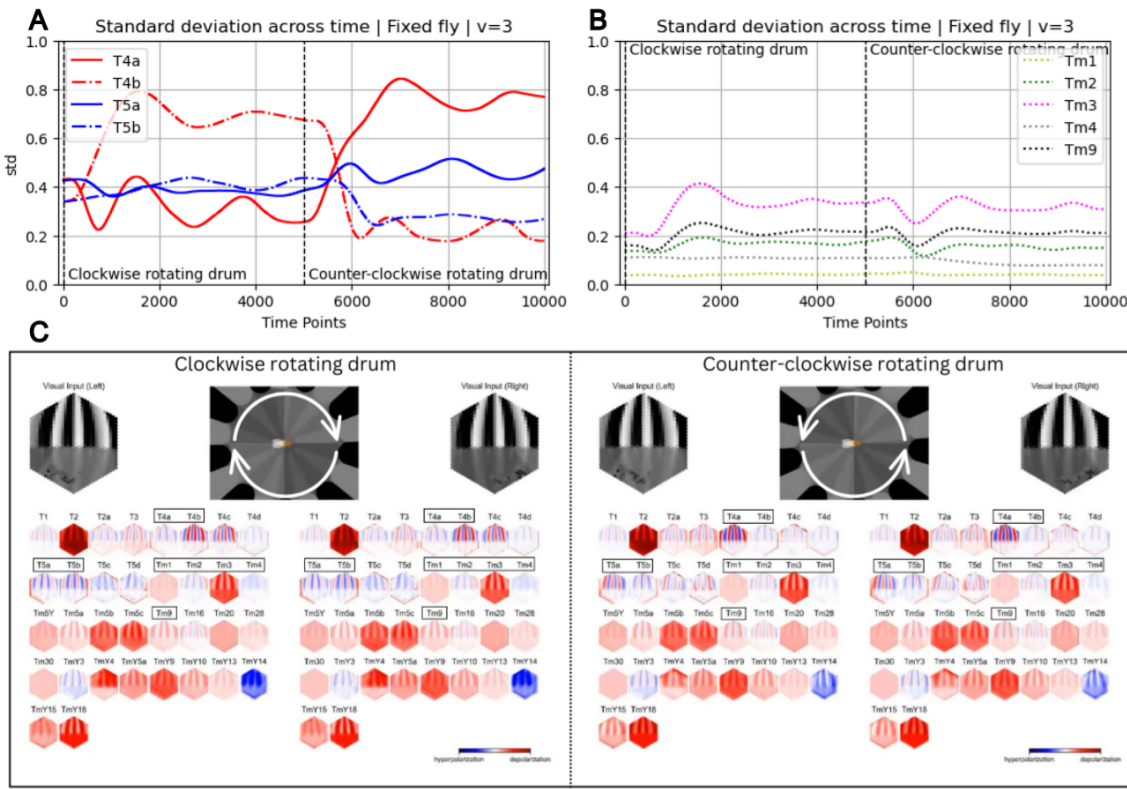


FIGURE 8

Neuronal activity patterns in the presence of a rotating striped drum over time. **A|** Evolution of T4a (ON leftward), T4b (ON rightward), T5a (OFF leftward), and T5b (OFF rightward) standard deviations across time. **B|** Evolution of Tm1, Tm2, Tm3, Tm4, and Tm9 standard deviations across time. All activities are displayed for a fixed fly with a drum rotating at a speed v equal to 3 radians/second. **C|** Snapshots of the video rendering of the optomotor reaction simulation for a clockwise and counter-clockwise rotation of the striped drum.

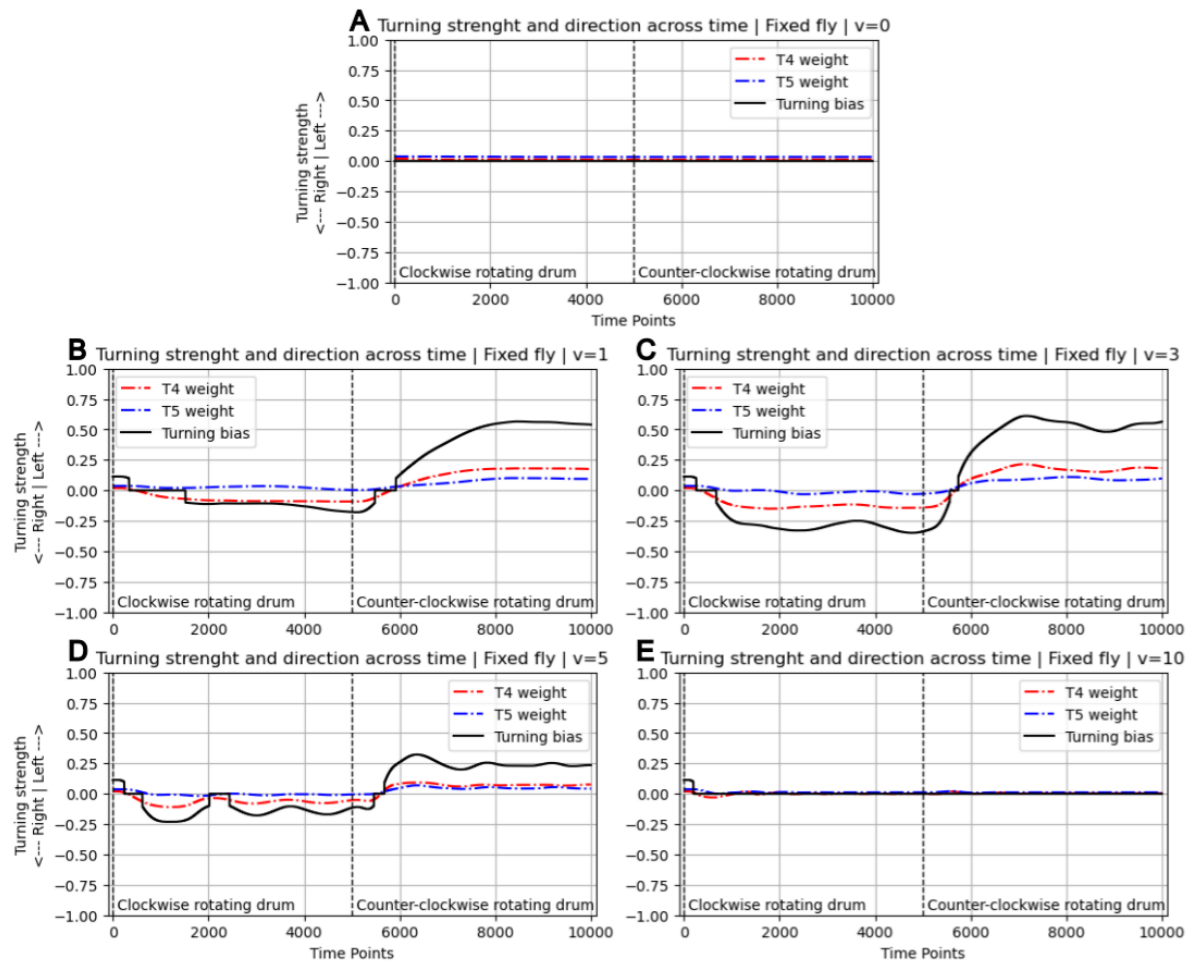


FIGURE 9

Evolution of T4 weight, T5 weight, and turning bias strength (equation 1) over time as a striped drum rotates at varying speeds. The drum rotates at a speed v equal to 0 (**A**), 1 (**B**), 3 (**C**), 5 (**D**), or 10 radians/second (**E**), clockwise from time $t=1$ to $t=5000$, and then counter-clockwise until $t=10000$. The simulation uses the full equation 1 while the fly is kept fixed. T4 weight and T5 weight correspond, respectively, to the left-hand side and right-hand side of the equation.

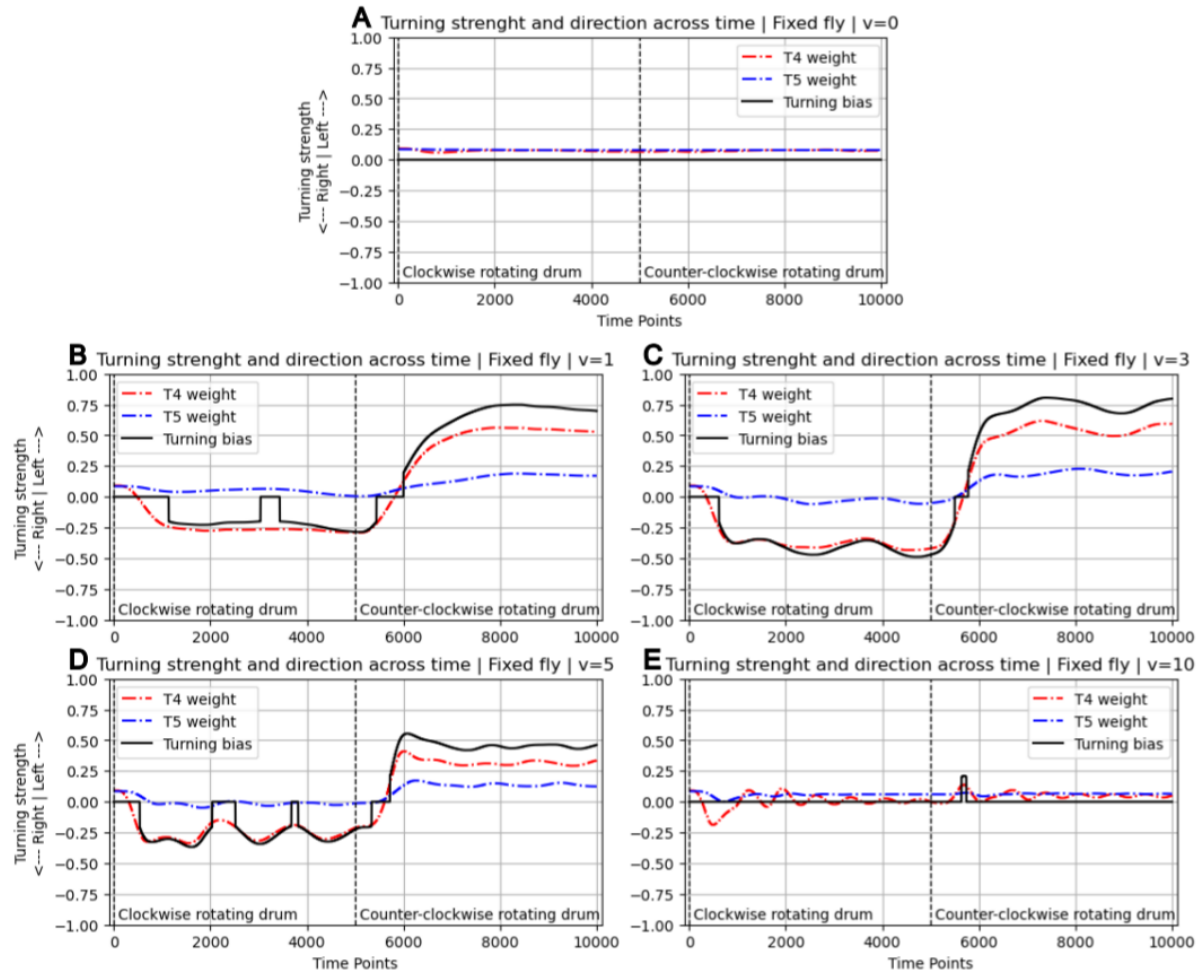


FIGURE 10

Evolution of T4 weight, T5 weight, and turning bias strength (equation 2) over time as a striped drum rotates at varying speeds. The drum rotates at a speed v equal to 0 (**A**), 1 (**B**), 3 (**C**), 5 (**D**), or 10 radians/second (**E**), clockwise from time $t=1$ to $t=5000$, and then counter-clockwise until $t=10000$. The simulation uses the equation 2 without T_m neurons while the fly is kept fixed. T4 weight and T5 weight correspond, respectively, to the left-hand side and right-hand side of the equation.

3.1.2 APPROACHING OBJECT

In a similar manner as above, we analyzed individual neuron responses to a looming stimulus (see Fig. 11 and supplementary video V4). However, as the visual scene perceived by both eyes was dissimilar, we have not used the equations presented in Section 2.3 for further analysis of neuronal patterns. Instead of averaging the ommatidia std over both eyes, we have calculated the difference of ommatidia std across eyes (see Fig. 12).

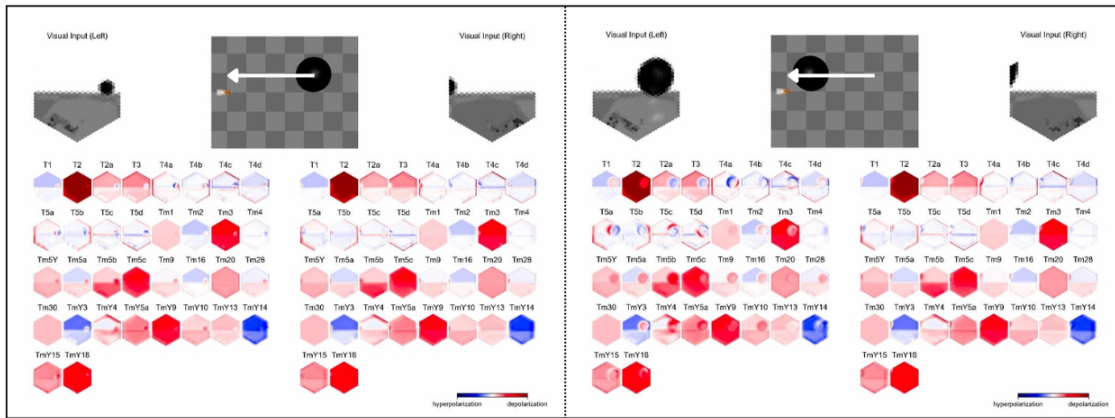


FIGURE 11

Snapshots of the video rendering of the looming reaction simulation for an approaching object at a speed v equal to 10 (a.u.). The dark object is slightly off-centered compared to the fly and moves toward the insect at a constant speed.

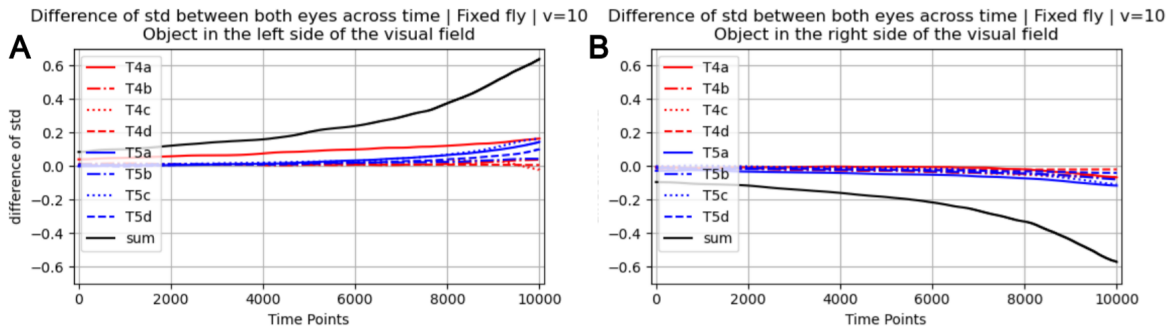


FIGURE 12

Evolution of the neuronal activity standard deviation differences between both eyes. The red and blue curves correspond respectively to T4 and T5 std differences, and the black curve corresponds to their sum. The object is either initialized on the left side (**A**) or the right side (**B**) of the visual field of the fly.

3.2 OPTOMOTOR RESPONSE IN REAL TIME (LARGE-FIELD ROTATING STIMULI)

Now that we know how neurons behave in a fixed fly, we use their output in real time to control the fly through the turning bias. We have generated 4 types of behavior (see Fig. 13 and supplementary videos V5, V6, V7, and V8, respectively):

- optomotor turning using the full equation 1 in an adaptative manner (3),
- optomotor turning using the equation 2 without Tm neurons in an adaptative manner (3),
- optomotor turning using the full equation 1 in an all-or-none manner (4),
- optomotor turning using the equation 2 without Tm neurons in an all-or-none manner (4),

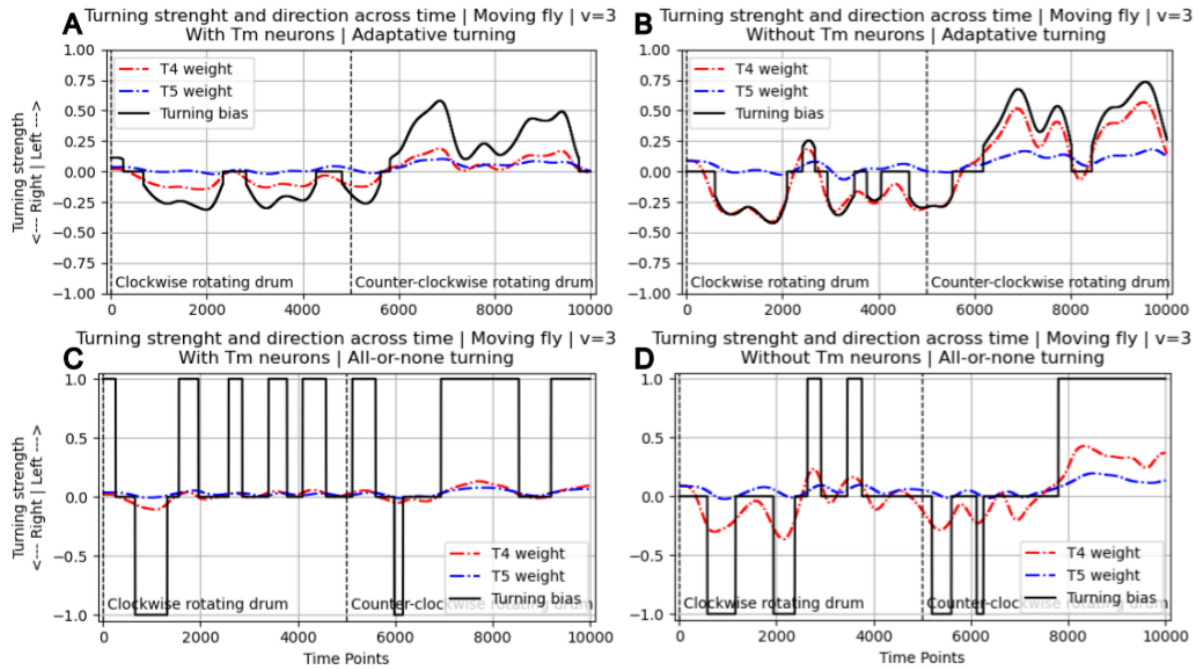


FIGURE 13

Evolution of T4 weight, T5 weight, and turning bias strength over time for a striped drum rotating at a speed equal to 3 radians/second. The turning of the fly is either controlled in an adaptive manner using equation 3 (**A, B**) or in an all-or-none manner using equation 4 (**C, D**). The optomotor response was generated using the full equation 1 (**A, C**) or the equation 2 without Tm neurons (**B, D**). The drum rotates clockwise from time $t=1$ to $t=5000$, and then counter-clockwise until $t=10000$. T4 weight and T5 weight correspond, respectively, to the left-hand side and right-hand side of the corresponding equation.

4 DISCUSSION

4.1 THE ADAPTATIVE CONTROLLER YIELDS BETTER RESULTS THAN THE ALL-OR-NONE CONTROLLER

We have implemented two main types of optomotor controllers. The adaptative controller (based on equation 1) allows to regulate the fly's turning speed according to the rotational velocity of the striped drums. Conversely, the all-or-none controller (based on equation 2) preserves the turning direction but uses a constant speed. As observed in figure 13, the adaptative controller yields the best results. In particular, we observed that the fly sometimes turns in the wrong direction when using the other controller. An explanation could be that, for a short period of time, the fly turns too fast compared to its environment, generating a visual motion in the opposite direction.

For example, when the drum starts rotating clockwise, the neurons with the corresponding preferred direction, in this case T4b and T5b neurons, become highly activated (which generates large std values), eliciting a rightward turn. But as the fly rotates, it perceives the environment as being static, or even rotating in the opposite direction if the fly velocity is too high. By using the adaptative controller, it prevents the fly from turning faster than its environment.

It is also important to note that the controller was not optimized to keep the fly in the center

of the arena, and we observed that, as it was turning, it made some steps forward. Therefore, with simulations running over longer periods of time, the fly might, at some point, touch the wall of the rotating drum. We have not been able to keep the fly in place, but one strategy could be to use an asymmetrical turning bias. For example, a turning bias equal to [1.2, -0.4] can successfully induce a rightward turn in the fly while limiting forward displacement. Further work could involve optimizing the controller to reproduce similar turning patterns in an adaptive manner.

4.2 ONLY A FEW NEURONS ARE REQUIRED TO GENERATE COMPLEX BEHAVIORS

We built the full equation 1 of the optomotor controller based on work available in the literature [5]. With only 9 neuron types, we managed to generate an optomotor response in the biomechanical fly. However, we observed that T4a and T4b neurons were the main drivers of the turning strength, as T5a and T5b displayed similar activities (thus similar std values as shown in figure 8) regardless of the direction of the motion. For this reason, the black curves of the turning bias from figures 9 and 10 highly resemble the red curves of the perceived motion direction by T4 neurons.

Unlike T4 and T5 neurons, Tm neurons do not hold any directional or velocity information. However, we have observed slight changes in activity in some of them (namely Tm2, Tm3, and Tm9) when the direction of the rotating drum changes. Specifically, they could have a role in stabilizing the optomotor response of the fly by reducing oscillation amplitudes in the turning strength. As a result, the turning strength is decreased, but the rotation is smoother.

4.3 DIRECTIONAL BIAS FOR LEFTWARD MOTION

In most of the results presented previously (and particularly in figure 8), we have observed that a leftward motion generates stronger activity changes in T4a and T5a neurons than a rightward motion does in T4b and T5b neurons. As a result, the strength to generate a leftward turn is generally stronger than what is required for a rightward turn.

It is important to note that, while the drums first rotate clockwise and then counter-clockwise in all the simulations, this sequence is not the cause of the bias. Indeed, inverting the sequence (counter-clockwise rotation followed by clockwise rotation) did not reverse the bias. A possible explanation could be that the network was trained mostly on visual inputs displaying motion patterns from right to left, thus creating a 'preference' for leftward motion, but further investigation is required.

Another directional bias relevant to mention is the simultaneous and similar changes in activity from T4b and T4c neurons, even though they should be tuned to different directions (respectively rightward and upward). This could come from the distorted field of vision of the fly: the insect might perceive vertical motion in its peripheral field of view even though the bars strictly move horizontally.

4.4 ANGULAR VELOCITY LIMITS

In the results obtained for the immobile fly with the rotating drum, it becomes easy to notice that starting at an angular velocity of 5 radians/second, some neurons (namely Tm4, T4d, T1,

and Tm5Y) start displaying an attenuated activity in response to the moving stimulus (see supplementary video V3), which only aggravates and extends to the other neurons as the rotation velocity increases (see supplementary video V9 for a rotational speed of 10 radians/second). Because of this event, the controller does not obtain any relevant input, and the optomotor response does not take place.

This comes as a surprise, as we had been able to induce aliasing in the fly in the exercise session of week 4 (see code). To do so, according to the Nyquist-Shannon Sampling Theorem [20] we should have: $f_s < 2f_d$ with f_s the sampling frequency, given by the eye of the fly, set at 500Hz, and f_d the stimulus frequency. Looking at the calculation from Section 2.2.1, one can easily find the theoretical velocity limit of the drum to induce aliasing for such a model (about 174 radians/second). Empirically, we have found that it corresponded to a value between 3500 and 3750 radians/second (see supplementary videos V10 for 3500 rad/s and V11 for 3750 rad/s), which is much higher.

Independently, we can see that no matter the velocity of the stimulus, the fly's eyes are able to capture it and perform its integration with the Hassenstein-Reichardt correlator. Even though we found an empirical maximal velocity for the capacity of the neuron network much smaller than what was predicted in Section 2.2.1, this issue with the neurons' activities might come from the training of the connectome-constrained neural network used, which was performed on videos of 24 fps, along with resampling and interpolation of the optic flow.

4.5 LOOMING STIMULI

Rotating striped drums and approaching shadows are two very distinct visual stimuli that elicit different behaviors, namely an optomotor and an escape response. While we have implemented a controller to generate an optomotor response, we have not implemented an equivalent to trigger an escape. In this section, we propose a strategy for such an implementation.

In Section 3.1.2, we have observed that when a black object approaches the fly and is off-center relative to the insect, the visual stimuli perceived by both eyes differ significantly. By analyzing the neuronal activity patterns resulting from both eyes, particularly summing the standard deviation differences across eyes in T4 and T5 neurons, we can determine the direction from which the object approaches by looking at the sign of the sum, while its absolute value provides an estimation of the distance separating the object from the fly, as shown in figure 12. As the black object expands, all four directional sensitivities (rightward, leftward, upward, and downward) are relevant to consider.

To trigger an escape response, we could set a threshold representing the critical size of the object in the visual field of the insect. Once the sum of the std differences between both eyes reaches the threshold, it will generate a predefined sequence of movement simulating an escape in the appropriate direction. This strategy allows for quicker escapes in response to faster-approaching objects, mimicking the natural fly behavior. However, we expect this controller to work poorly in cases where the object is positioned exactly in front of the fly, as both eyes would capture the same (but mirrored) visual input.

Finally, it is important to note that an escape controller defined in this manner should be compatible with the optomotor controller we have defined in Section 2.3, and both could be implemented simultaneously in a single fly. Indeed, rotating striped drums generate similar visual stimuli in both eyes (thus neuronal patterns resulting from both eyes are equivalent), while objects approaching from one side do not. Therefore, looming stimuli would not trigger an

optomotor response, and conversely, rotational stimuli would not trigger an escape response.

4.6 ANTI-DIRECTIONAL TURNING

To trigger an optomotor response, we have used rotating drums with alternating black and white stripes. However, it could be interesting to observe the behavior of the fly when the stripes are less contrasted, for example, with alternating black and grey stripes. In particular, it has been shown that anti-directional optomotor turning (a reverse of the optomotor turning response over several seconds) is sometimes observed in *Drosophila* in the presence of high-contrast visual stimuli [21]. This could potentially explain the brief leftward turning of the fly when the drum starts rotating clockwise (as shown in figures 9 and 13), although it might be due to the fly needing to adjust its position at the beginning of the simulation. Further investigation is required as we were unable to change the color of white stripes to grey, and other cells than the ones considered in this study are thought to be involved in this behavior. Specifically, changing the color of some stripes could help determine if this is indeed an anti-directional turning behavior or if it is only due to the initialization of the fly in the environment. Otherwise, initiating the rotation of the striped drum at $t=1000$ instead of $t=1$ is another strategy to explore.

5 CONCLUSION

In this study, we have explored the integration of a connectome-constrained deep neural network with the NeuroMechFly 2.0 biomechanical model to simulate visually guided behaviors in the adult fly, *Drosophila melanogaster*. By taking advantage of the detailed anatomical and functional data of the fly’s visual system, we succeeded in eliciting the optomotor response, a key stabilization behavior that we could then analyze, as well as implementing the environment corresponding to looming, which would drive an escape response.

Our findings support the efficacy of the connectome-constrained network in processing visual information and generating realistic behavioral responses. The neural network, optimized to compute optic flow, successfully reproduced the visual motion processing seen in biological flies, although some training parameters might limit its performance to specific examples of motion.

We created two distinct experimental arenas to test the fly’s responses: a rotating striped drum for the optomotor response and an approaching object for the looming response (for which we did not implement the escape response). The simulations showed that varying the angular velocity of the rotating drum induced different patterns of neural activity in the fly’s retina, aligning with the expected behavior of T4 and T5 neurons.

Future work could expand on these findings by exploring the various datasets that could be used to train the neural network in order to study the effect on motion preference for left and right movements, as well as the gap between theoretical and empirical limit velocities for the network’s processing capacity or aliasing induction. Additionally, the approaching or looming stimulus could be further investigated with the computation of the escape response and the elaboration of a controller capable of generating both optomotor and looming responses.

REFERENCES

- [1] Sibo Wang-Chen et al. ‘NeuroMechFly 2.0, a framework for simulating embodied sensorimotor control in adult Drosophila’. In: *bioRxiv* (2023). DOI: 10.1101/2023.09.18.556649. URL: <https://www.biorxiv.org/content/early/2023/09/18/2023.09.18.556649>.
- [2] Victor Lobato-Rios et al. ‘NeuroMechFly, a neuromechanical model of adult Drosophila melanogaster’. In: *Nature Methods* 19.5 (May 2022), pp. 620–627. DOI: 10.1038/s41592-022-01466-7. URL: <https://doi.org/10.1038/s41592-022-01466-7>.
- [3] Selig Hecht and George Wald. ‘THE VISUAL ACUITY AND INTENSITY DISCRIMINATION OF DROSOPHILA’. In: *Journal of General Physiology* (1934).
- [4] Haritz Plazaola-Sasieta et al. ‘Untangling the wiring of the Drosophila visual system: developmental principles and molecular strategies’. In: *Journal of Neurogenetics* (2017).
- [5] Alexander Borst. ‘Fly visual course control: behaviour, algorithms and circuits’. In: *Nature Reviews Neuroscience* (2014).
- [6] Alexander Borst and Lukas Groschner. ‘How Flies Fee Motion’. In: *Annual Review of Neuroscience* (2023).
- [7] Upal Mahbub, Hafiz Imtiaz and Atiqur Ahad. ‘An optical flow based approach for action recognition’. In: *IEEE* (2012).
- [8] Brian Duistermars, Rachel Care and Mark Frye. ‘Binocular interactions underlying the classic optomotor responses of flying flies’. In: *Frontiers in Behavioral Neuroscience* (2012).
- [9] Lance Tammero, Mark Frye and Michael Dickinson. ‘Spatial organization of visuomotor reflexes in Drosophila’. In: *Journal of Experimental Biology* (2004).
- [10] Leesun Ryu, Sung Kim and Anmo Kim. ‘From Photons to Behaviors: Neural Implementations of Visual Behaviors in Drosophila’. In: *Frontiers in Neuroscience* (2022).
- [11] Väinö Haikala et al. ‘Optogenetic Control of Fly Optomotor Responses’. In: *Journal of Neuroscience* (2013).
- [12] Holmqvist and Srinivasan. ‘A visually evoked escape response of the housefly’. In: *Journal of Comparative Physiology A* (1991).
- [13] Jan Ache et al. ‘Neural Basis for Looming Size and Velocity Encoding in the Drosophila Giant Fiber Escape Pathway’. In: *Current Biology* (2019).
- [14] Timothy Dunn et al. ‘Neural Circuits Underlying Visually Evoked Escapes in Larval Zebrafish’. In: *Neuron* (2016).
- [15] Lance Tammero and Michael Dickinson. ‘Collision-avoidance and landing responses are mediated by separate pathways in the fruit fly, Drosophila melanogaster’. In: *Journal of Experimental Biology* (2002).
- [16] Michael Reiser and Michael Dickinson. ‘Drosophila fly straight by fixating objects in the face of expanding optic flow’. In: *Journal of Experimental Biology* (2010).
- [17] Janne K Lappalainen et al. ‘Connectome-constrained deep mechanistic networks predict neural responses across the fly visual system at single-neuron resolution’. In: *bioRxiv* (2023).
- [18] Daniel J. Butler et al. ‘A Naturalistic Open Source Movie for Optical Flow Evaluation’. In: *Computer Vision – ECCV 2012*. Ed. by Andrew Fitzgibbon et al. Berlin, Heidelberg: Springer Berlin Heidelberg, 2012, pp. 611–625. ISBN: 978-3-642-33783-3.

- [19] Emanuel Todorov, Tom Erez and Yuval Tassa. ‘MuJoCo: A physics engine for model-based control’. In: *2012 IEEE/RSJ International Conference on Intelligent Robots and Systems*. IEEE. 2012, pp. 5026–5033. DOI: [10.1109/IROS.2012.6386109](https://doi.org/10.1109/IROS.2012.6386109).
- [20] Claude Shannon. ‘Communication in the Presence of Noise’. In: *IEEE* (1949).
- [21] Omer Mano et al. ‘Long-timescale anti-directional rotation in Drosophila optomotor behavior’. In: *Neuron* (2016).